High-T_c Superconductivity near the Anion Height Instability in Fe-Based Superconductors: Analysis of $LaFeAsO_{1-x}H_x$

Seiichiro Onari,[1] Youichi Yamakawa,[2] and Hiroshi Kontani[2]
[1]Department of Applied Physics, Nagoya University, Furo-cho, Nagoya 464-8603, Japan
[2]Department of Physics, Nagoya University, Furo-cho, Nagoya 464-8602, Japan
(Received 7 December 2013; published 6 May 2014)

The isostructural transition in the tetragonal phase with a sizable change in the anion height, is realized in heavily H-doped LaFeAsO and (La,P) codoped $CaFe_2As_2$. In these compounds, the superconductivity with higher T_c (40–50 K) is realized near the isostructural transition. To find the origin of the anion-height instability and the role in realizing the higher-T_c state, we develop the orbital-spin fluctuation theory by including the vertex correction. We analyze $LaFeAsO_{1-x}H_x$ and find that the non-nematic orbital fluctuations, which induce the anion-height instability, are automatically obtained at $x \sim 0.5$, in addition to the conventional nematic orbital fluctuations at $x \sim 0$. The non-nematic orbital order triggers the isostructural transition, and its fluctuation would be a key ingredient to realize higher-T_c superconductivity of order 50 K.

DOI: 10.1103/PhysRevLett.112.187001 PACS numbers: 74.70.Xa, 74.20.Pq, 74.20.Rp

The normal-state phase diagram of Fe-based superconductors is important to reveal the essential electronic states and the mechanism of superconductivity. In many compounds, the structure transition from tetragonal (C_4) to orthorhombic (C_2) is realized at T_S, and the antiferromagnetic (AFM) order appears at T_N below T_S. The superconductivity is realized near the structural quantum critical point (QCP) at $T_S = 0$ and/or the magnetic QCP at $T_N = 0$. For example, the optimum T_c in $FeSe_xTe_{1-x}$ is realized near the structural QCP at $x \approx 0.6$ [1], whereas AFM order is absent for $x > 0.5$.

To explain the C_2 structure transition, both the spin-nematic [2] and orbital-nematic [3–7] mechanisms have been proposed. In the latter scenario, orbital-nematic order is induced by spin fluctuations due to strong orbital-spin mode coupling described by the vertex correction (VC) [6]. Both mechanisms can explain the shear modulus C_{66} softening [8,9]. The orbital mechanism would be consistent with the large d-level splitting $E_{yz} - E_{xz} \sim 500$ K in the C_2 phase [10,11] and with the large orbital susceptibility given by Raman spectroscopy [12,13]. The nematic order is observed by the magnetic torque measurements [14]. Since the superconductivity is realized next to the orbital and spin ordered phases, both fluctuations would be essential for the pairing mechanism.

However, this is not the whole story of Fe pnictides: The unique phase diagram of $LaFeAsO_{1-x}H_x$ with double-dome superconducting phase [15,16] attracts great attention. The second superconducting dome ($x \geq 0.2$) is next to the "C_4 isostructural phase transition" with sizable change in the c-axis length (or anion height) for $0.45 < x < 0.5$ [17,18]. (The c-axis length is unchanged in the C_2 structure transition at $x \sim 0$.) Similarly, high-T_c (~50 K) superconductivity is realized near the "collapsed C_4 phase" in rare-earth doped $CaFe_2As_2$ [19,20]. In (La,P) codoped $CaFe_2As_2$, a higher-T_c state is realized near the anion-height instability, whereas it avoids the AFM phase as clearly shown in Refs. [19,20]. These experiments strongly indicate that the anion-height instability is a key ingredient for higher-T_c superconductivity of order 50 K. The authors in Ref. [21] discussed that the C_4 phase in $(Ba,Na)Fe_2As_2$ originates from the C_4 magnetic order. However, stripe magnetic order ($= C_2$ symmetry) is realized in $LaFeAsO_{1-x}H_x$ at $x \sim 0.5$ [17], which indicates small spin-lattice coupling.

In this Letter, we discuss the origin of the anion-height instability and its role of higher-T_c superconductivity. For this purpose, we study $LaFeAsO_{1-x}H_x$ ($x = 0 \sim 0.5$) by calculating both the VC and the self-energy Σ self-consistently. By this "self-consistent VC + Σ (SC-VC_Σ) method," we obtain the non-nematic orbital order $O_{3z^2-r^2}$ at $x \sim 0.5$. This order parameter couples to the anion-height change and triggers the C_4 isostructural transition, which cannot be explained by the spin-fluctuation theories without the VC [22–24]. We also find that the orbital-fluctuation-mediated s-wave state is stabilized by including the VC for the gap equation, which is dropped in conventional Migdal-Eliashberg theory. The present study reveals that multiple kinds of orbital fluctuations play significant roles in Fe-based superconductors.

Figure 1(a) shows the phase diagram of $LaFeAsO_{1-x}H_x$: We propose that the charge quadrupole order $O_{3z^2-r^2} \equiv \frac{1}{2}(n_{xz} + n_{yz}) - n_{xy}$ ($O_{x^2-y^2} \equiv n_{xz} - n_{yz}$) appears at $x \sim 0.5$ ($x \sim 0$). The softening of the longitudinal modulus along the c axis C_{33} observed in under- and overdoped $Ba(Fe_{1-x}Co_x)_2As_2$ [25] indicates that $O_{3z^2-r^2}$ quadrupole fluctuations exist in various Fe-based compounds.

The tight-binding model of $LaFeAsO_{1-x}H_x$ for $0 \leq x \leq 0.5$ was introduced by the present authors in Ref. [15]. The

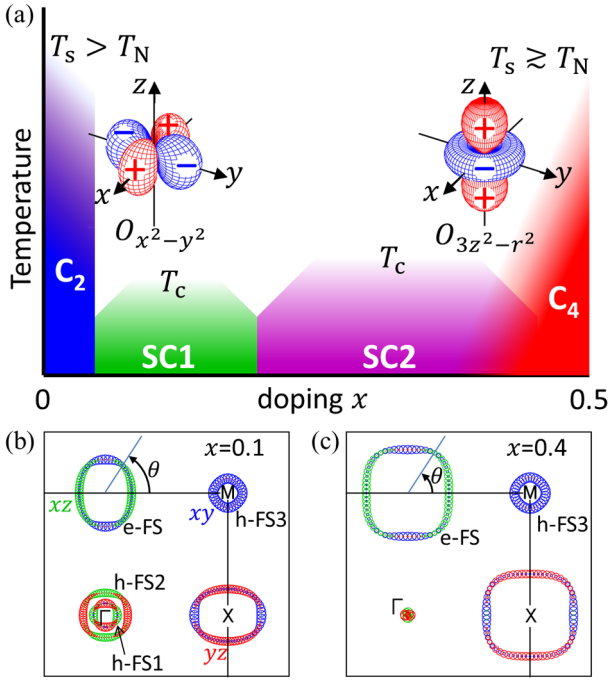

FIG. 1 (color online). (a) Schematic phase diagram of $LaFeAsO_{1-x}H_x$. We predict that non-nematic $O_{3z^2-r^2}$ (nematic $O_{x^2-y^2}$) charge quadrupole order emerges in the C_4 (C_2) phase. (b),(c) FSs at $x = 0.1$ and $x = 0.4$ [22]. e-FS is the electron pocket and h-FS3 (h-FS1, 2) is the hole pocket composed of the d_{xy} (d_{xz}, d_{yz}) orbital.

Fermi surfaces (FSs) for $x = 0.1$ and 0.4 are shown in Figs. 1(b) and 1(c), respectively. The intraorbital nesting and interorbital one are the driving forces of the magnetic and orbital fluctuations, respectively. We analyze the multiorbital Hubbard model with intra- (inter)orbital interaction U (U') and the exchange interaction J under the constraint $U = U' + 2J$, assuming uniform states. Electronic phase separation due to the imperfect nesting is discussed in Ref. [26].

Here, we denote $d_{3z^2-r^2}$, d_{xz}, d_{yz}, d_{xy}, $d_{x^2-y^2}$ orbitals as 1,2,3,4,5. The FSs are mainly composed of 2,3,4 orbitals. The charge (spin) susceptibility $\hat{\chi}^{c(s)}(q)$ is given in the $5^2 \times 5^2$ matrix form in the orbital basis as follows:

$$\hat{\chi}^{c(s)}(q) = \hat{\Phi}^{c(s)}(q)[1 - \hat{\Gamma}^{c(s)}\hat{\Phi}^{c(s)}(q)]^{-1}, \qquad (1)$$

where $q = (\boldsymbol{q}, \omega_l)$ and $\hat{\Phi}^{c(s)}(q) = \hat{\chi}^{(0)}(q) + \hat{X}^{c(s)}(q)$: $\hat{\chi}^{(0)}(q)$ is the bubble susceptibility with self-energy correction, and $\hat{X}^{c(s)}(q)$ is the VC for charge (spin) channel. $\hat{\Gamma}^{c(s)}$ is the matrix form of the bare Coulomb interaction for the charge (spin) sector [27]. In the original SC-VC_Σ method, the VC is given by the Maki-Thompson and Aslamazov-Larkin (AL) terms, which are the first- and second-order terms, respectively, with respect to $\hat{\chi}^{c,s}$. Since $\hat{X}^c \gg \hat{X}^s$ near the QCP, we put $\hat{X}^s(q) = 0$ and calculate only the AL term for $\hat{X}^c(q)$ self-consistently. Its justification is verified in Refs. [6,28] and also confirmed by the recent renormalization group study [29].

The charge (spin) Stoner factor $\alpha_{c(s)}$ is given by the maximum eigenvalue of $\hat{\Gamma}^{c(s)}\hat{\Phi}^{c(s)}(q)$ in Eq. (1), and $\alpha_{c(s)} = 1$ corresponds to the orbital (spin) order. Although the relation $\alpha_s \gg \alpha_c$ is satisfied within the RPA for $J > 0$, the opposite relation can be realized if the VC is taken into account beyond the RPA. Here, we introduce the quadrupole susceptibilities:

$$\chi^Q_\gamma(\boldsymbol{q}, \omega_l) = \sum_{l,l',m,m'} O^{l,l'}_\gamma \chi^c_{l,l';m,m'}(\boldsymbol{q}, \omega_l) O^{m',m}_\gamma, \qquad (2)$$

where $\gamma = x^2 - y^2$, $3z^2 - r^2$, xz, yz, xy represents the quadrupole [30]. Then, $\chi^Q_{x^2-y^2}(q) \approx \chi^c_{2,2;2,2}(q) + \chi^c_{3,3;3,3}(q) - 2\chi^c_{2,2;3,3}(q)$ and $\chi^Q_{3z^2-r^2}(q) \approx \chi^c_{4,4;4,4}(q) - \sum_{l=2,3}\chi^c_{l,l;4,4}(q) + \sum_{l,m=2,3}\chi^c_{l,l;m,m}(q)/4$.

Now, we study the tight-binding Hubbard models of $LaFeAsO_{1-x}H_x$ based on the SC-VC_Σ method, in which both the VC and the one-loop self-energy $\hat{\Sigma}$ are calculated self-consistently. By this method, the mass-enhancement factor for the l orbital is given as $1/z_l = 1 - \mathrm{Re}d\Sigma_l(k, \omega)/d\omega|_{\omega=0}$, and we obtain $1/z_l = 3$–5 for $l = 2$–4 and $1/z_4 > 1/z_{2,3}$ in $LaFeAsO_{1-x}H_x$. The expressions of the VC and $\hat{\Sigma}$ are explained in Ref. [31] in detail. Hereafter, we fix the parameters $J/U = 0.14$ and $T = 0.05$ eV, and the unit of energy is eV.

Figure 2 shows the largest two static quadrupole susceptibilities $\chi^Q_\gamma(\boldsymbol{q})$ for Fig. 2(a) $x = 0$ and Fig. 2(b) $x = 0.4$, respectively. For each x, the relations $\alpha_c = 0.97$ and $a_c > \alpha_s \sim 0.9$ are satisfied consistently with the relation $T_S > T_N$. At $x = 0$ in Fig. 2(a), we obtain the strong developments of $\chi^Q_{x^2-y^2}(\boldsymbol{0})$ and $\chi^Q_{xz}(\boldsymbol{Q})$, similar to the previous

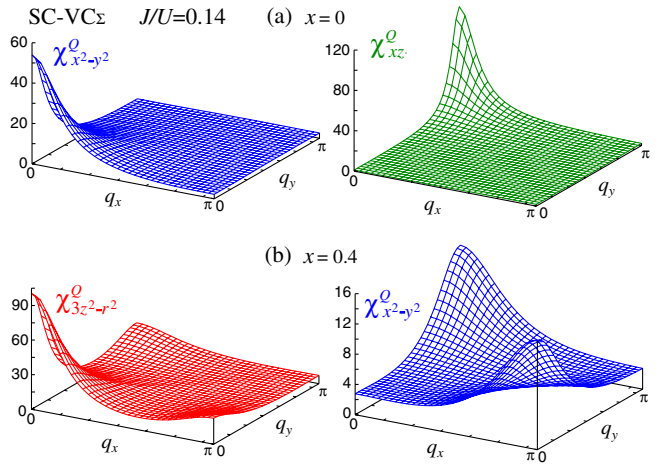

FIG. 2 (color online). $\chi^Q_\gamma(\boldsymbol{q})$ at zero frequency obtained by the SC-VC_Σ method: (a) $\gamma = x^2 - y^2$ and $\gamma = xz$ for $x = 0$ ($U = 2.06$) and (b) $\gamma = 3z^2 - r^2$ and $\gamma = x^2 - y^2$ for $x = 0.4$ ($U = 1.68$). Note that $\chi^Q_{xz}(q_x, q_y) = \chi^Q_{yz}(q_y, q_x)$. Similar results are obtained by the SC-VC method [32].

SC-VC analysis [6]. The divergence of $\chi^{Q}_{x^2-y^2}(\mathbf{0})$ causes the C_2 structure transition. In addition, large antiferro-orbital fluctuations are induced by the cooperation of the VC and the good interorbital nesting between the e-FS and h-FSs [6]. The shear modulus $C_{66} \propto 1 - g_{x^2-y^2}\chi^{Q}_{x^2-y^2}(\mathbf{0})$ reaches zero even if $\chi^{Q}_{x^2-y^2}(\mathbf{0})$ in the SC-VC$_\Sigma$ method is finite, where $g_{x^2-y^2}(\ll 1)$ is the quadrupole interaction due to the acoustic phonon [33].

At $x = 0.4$ in Fig. 2(b), in contrast, we obtain the large peak of $\chi^{Q}_{3z^2-r^2}(\mathbf{0})$ due to the VC. Since its divergence induces the change in the ratio n_{xy}/n_{xz} while keeping $n_{xz} = n_{yz}$, the obtained large $\chi^{Q}_{3z^2-r^2}(\mathbf{0})$ gives the nonnematic (C_4) orbital fluctuations and anion-height instability. In addition, large antiferro-orbital fluctuations $\chi^{Q}_{x^2-y^2}(\boldsymbol{Q})$ are also induced by the VC. It is noteworthy that a strong interorbital charge transfer from in-plane to out-of-plane orbitals is observed in Co-doped $BaFe_2As_2$ [34].

Here, we try to understand the orbital-spin mode coupling due to the AL term in terms of the localized picture $U \gg W_{\rm band}$: First, we introduce the Kugel-Khomskii (KK)-type orbital-dependent exchange interaction [35] between the nearest-neighbor d_{xz}, d_{yz} orbitals, $H' \sim J^{(1)} \sum^{\rm NN}_{\langle i,j\rangle} (\boldsymbol{s}_i \cdot \boldsymbol{s}_j)(n^i_{xz} n^j_{xz} \delta_{i-j,(\pm 1,0)} + n^i_{yz} n^j_{yz} \delta_{i-j,(0,\pm 1)})$, as shown in Fig. 3(a). Note that $J^{(1)} \sim 2t^2/U$. Because of this orbital-spin coupling term, if the AFM order with $\boldsymbol{Q} = (\pi, 0)$ is realized, the electrons at each site will occupy the d_{xz} orbital, as shown in Fig. 3(a). That is, the AFM order or fluctuations induce the C_2 orbital order ($n_{xz} \neq n_{yz}$) or fluctuations and vice versa. Next, we consider the single d_{xy}-orbital model with the nearest- and next-nearest-neighbor exchange interactions: $H'' \sim J^{(1)}_{xy} \sum^{\rm NN}_{\langle i,j\rangle} (\boldsymbol{s}_i \cdot \boldsymbol{s}_j)(n^i_{xy} n^j_{xy}) + J^{(2)}_{xy} \sum^{\rm NNN}_{\langle i,j\rangle} (\boldsymbol{s}_i \cdot \boldsymbol{s}_j)(n^i_{xy} n^j_{xy})$. When $J^{(2)}_{xy} > \frac{1}{2} J^{(1)}_{xy}$, the $\boldsymbol{Q} = (\pi, 0)$ AFM state in Fig. 3(b) appears due to the "order-by-disorder" mechanism [36].

Now, we consider the three-orbital model $H' + H''$: When $J^{(2)}_{xy} \gg J^{(1)}$, the ferro-orbital polarization $n_{xy} \gg n_{xz} = n_{yz}$ with AFM order shown in Fig. 3(b) would be realized to gain the exchange energy. In this case, the AFM order or fluctuations induce non-nematic C_4 orbital order or fluctuations and vice versa. This case corresponds to $x \sim 0.5$ with strong d_{xy}-orbital spin fluctuations. Thus, the KK-type spin-orbital coupling is understandable in terms of the weak-coupling approach by including the AL term. The strong-coupling approaches are useful to understand the ordered phases [37].

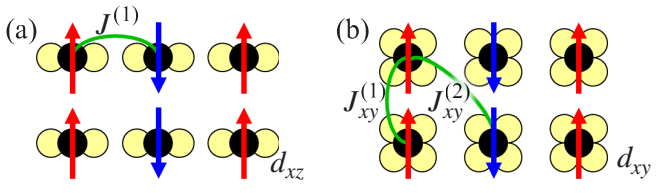

FIG. 3 (color online). (a) Localized (d_{xz}, d_{yz})-orbital model with KK coupling. (b) Localized d_{xy}-orbital model with Heisenberg coupling. Here, the occupied orbitals are shown.

We also discuss why the VC induces the C_4 (C_2) order at $x = 0.5$ ($x = 0$) analytically: When spin fluctuations develop mainly in the l orbital, the charge AL term $X^c_{l,l;l,l}(\mathbf{0}) \sim T\sum_k \{\chi^s_{l,l;l,l}(k)\}^2$ becomes large [6,28]. Now, we analyze $\chi^{Q}_{\gamma}(\mathbf{0})$ by inputting only three irreducible susceptibilities $\Phi^c_l \equiv \chi^{(0)}_{l,l;l,l}(\mathbf{0}) + X^c_{l,l;l,l}(\mathbf{0})$ ($l = 2$–4) into Eq. (1). For $J = 0$, for simplicity, we obtain [28,32]

$$\chi^{Q}_{x^2-y^2}(\mathbf{0}) = 2\Phi^c_2(1 - U\Phi^c_2)^{-1}, \tag{3}$$

$$\chi^{Q}_{3z^2-r^2}(\mathbf{0}) = b(1 - aU\Phi^c_4)^{-1}, \tag{4}$$

where $a \equiv (5U\Phi^c_2 - 1)/(3U\Phi^c_2 + 1)$ and $b \sim (5U\Phi^c_4 + 1)^2/16U^2\Phi^c_4$ near the QCP. In the case of $\Phi^c_2 = \Phi^c_3 > a\Phi^c_4$, then $\chi^{Q}_{x^2-y^2}(\mathbf{0})$ is the most divergent. In the opposite case, $\chi^{Q}_{3z^2-r^2}(\mathbf{0})$ is the most divergent if a is positive. At $x \sim 0.4$, h-FS1 and h-FS2 almost disappear as shown in Fig. 1(c), so d_{xy}-orbital spin fluctuations become dominant [22]. For this reason, at $x \sim 0.4$, the $O_{3z^2-r^2}$ order and anion-height instability are driven by Φ^c_4 due to strong d_{xy}-orbital spin fluctuations.

Now, we study the superconductivity due to orbital and spin fluctuations based on the SC-VC$_\Sigma$ method. In almost all previous studies, the VC for the gap equation (Δ-VC) had been dropped. In strongly correlated systems, however, Δ-VC could be quantitatively important since Migdal's theorem is not valid anymore. Since the AL-type VC for $\chi^{Q}_{\gamma}(q)$ is very large, Δ-VC due to the AL-type diagram should be significant. Here, we solve the following gap equation in the orbital basis by taking the Δ-VC into account:

$$\lambda_E \Delta_{l,l'}(k) = -T\sum_{q,m_i} V_{l,m_1;m_4,l'}(k,q) G_{m_1,m_2}(q) \times \Delta_{m_2,m_3}(q) G_{m_4,m_3}(-q), \tag{5}$$

where λ_E is the eigenvalue, $\Delta_{l,l'}(k)$ is the gap function, and $G_{l,l'}(q)$ is the Green function with self-energy. The pairing interaction $V_{l,m_1;m_4,l'}(k,q)$ is given as

$$\hat{V}(k,q) = \frac{3}{2}\hat{\Lambda}^s(k,q)\hat{\Gamma}^s\hat{\chi}^s(k-q)\hat{\Gamma}^s\hat{\Lambda}'^s(-k,-q) - \frac{1}{2}\hat{\Lambda}^c(k,q)\hat{\Gamma}^c\hat{\chi}^c(k-q)\hat{\Gamma}^c\hat{\Lambda}'^c(-k,-q) + V^{(1)}, \tag{6}$$

where $\hat{\Lambda}^{c(s)}(k,q)$ is the vertex for the charge (spin) channel shown in Fig. 4(a), $\Lambda'^{c(s)}_{l,l';m,m'}(k,q) = \Lambda^{c(s)}_{m',m;l',l}(k,q)$, and $V^{(1)} = \frac{1}{2}(\hat{\Gamma}^s - \hat{\Gamma}^c) \sim U$. To be consistent with the SC-VC$_\Sigma$ method, we calculate the AL-type contribution to $\hat{\Lambda}^c(k,q)$ given in Fig. 4(b), whereas we put $\hat{\Lambda}^s(k,q) = \hat{1}$.

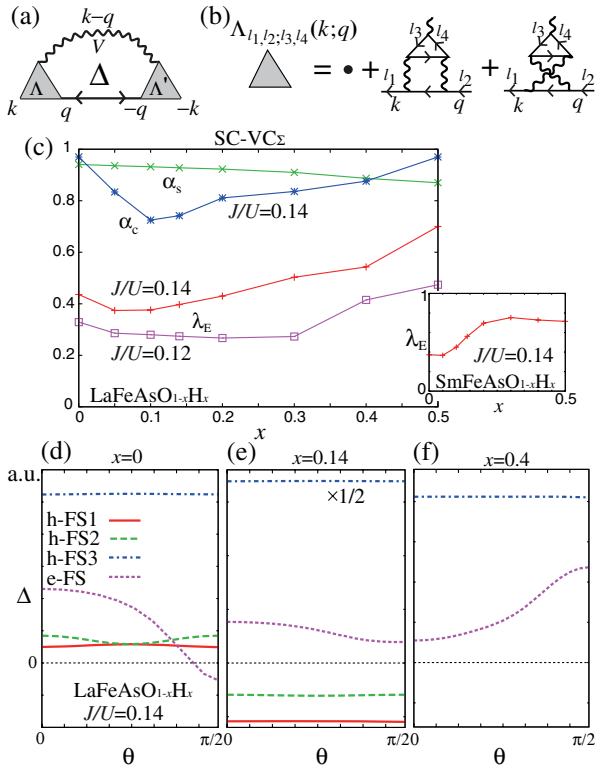

FIG. 4 (color online). (a) Gap equation with Δ-VC and (b) AL-type diagram for Λ. (c) $\alpha_{c,s}$ and λ_E as functions of x in $LaFeAsO_{1-x}H_x$ for $J/U = 0.14$. λ_E for $J/U = 0.12$ is also shown. (Inset: λ_E in $SmFeAsO_{1-x}H_x$.) The gap functions on the FSs at (d) $x = 0$, (e) $x = 0.14$, and (f) $x = 0.4$ for $J/U = 0.14$. θ is the azimuthal angle in Figs. 1(b) and 1(c).

To study the superconducting state for $x = 0$–0.5, we introduce $\bar{U}(x)$ by the linear interpolation between $U_c = 2.06$ at $x = 0$ and $U_c = 1.55$ at $x = 0.5$, as done in Ref. [22]. The obtained $\bar{U}(x)$ decreases with x, which will be given by the change in the Kanamori screening, which is dropped in the present one-loop Σ. In fact, the density of states at the Fermi level $N(0)$ increases by 30% by changing x from 0 to 0.5. In contrast, $\bar{U}(x)$ is a strong increasing function in the rigid band approximation [22]. Figure 4(c) shows the obtained x dependence of the $\alpha_{c,s}$ and λ_E for $J/U = 0.14$ by using $U = \bar{U}(x)$. The large α_c at $x = 0$ and that at $x = 0.5$ explain the experimental C_2 and C_4 structure transitions of $LaFeAsO_{1-x}H_x$. The eigenvalue λ_E approximately follows α_c and shows two peaks near the C_2 and C_4 structure transition points, due to the strong orbital fluctuations. Since T_c is suppressed by the structure transition, the obtained x dependence of λ_E would be consistent with the double-dome T_c. In contrast, single-dome T_c is obtained in the FLEX approximation in the present model [32].

Figures 4(d)–4(f) show the gap functions multiplied by z_l in the band basis for $x = 0$, 0.14, and 0.4, respectively. At $x \sim 0$ and 0.4, approximate s_{++}-wave states are obtained as shown in Figs. 4(d) and 4(f), due to the strong orbital fluctuations. At $x \sim 0.4$, the gap structure is fully gapped, whereas the gap on the e-FS is nodal at $x \sim 0$ due to the competition (cooperation) of orbital and spin fluctuations [38]. These s_{++}-type gap structures are realized by taking the Δ-VC into account beyond Migdal's theorem, since the attractive interaction due to $\hat{\chi}^c$ in Eq. (6) is multiplied by $|\hat{\Lambda}^c(k,q)|^2 \gg 1$ [6,31]. [The Δ-VC can overcome the factor 3 for the spin channel in Eq. (6) that favors the $s_\pm$ state.] The s_{++} state is realized against the strong Coulomb repulsion due to the retardation effect, since the energy scale of orbital fluctuations is $\sim T$. The s_{++} state is consistent with the robustness of T_c against the randomness in Fe pnictides [39–44].

Figure 4(e) shows the gap functions for $x = 0.14$. Although the spin fluctuation is stronger because of the relation $\alpha_c \ll \alpha_s$, the obtained gap structure is very different from the so-called $s_\pm$-wave state [45–47], in which the gaps of the three hole-FSs are the same in sign. This gap structure is induced by the cooperation of the "attractive interaction between h-FS3 and e-FS" due to orbital fluctuations and "repulsive interaction between h-FS1, 2 and e-FS" due to spin fluctuations [31]. This gap structure may easily change to the s_{++}-wave state by introducing a small amount of impurities and e-ph interaction [42].

We also performed the similar analysis for $SmFeAsO_{1-x}H_x$, which shows the single-dome T_c by constructing the first-principle tight-binding models. In Sm compounds, h-FS3 is very large due to the higher anion height [48], and the inter- and intraorbital nesting are improved. Since the strong orbital fluctuations appear even at $x \sim 0.2$, λ_E of $SmFeAsO_{1-x}H_x$ becomes larger, as shown in the inset of Fig. 4(c), and the single-dome T_c structure is well reproduced. This result indicates the importance of the d_{xy}-orbital FS to realize higher T_c.

In summary, we studied the phase diagram of $LaFeAsO_{1-x}H_x$ using the SC-VC_Σ method and predicted that the non-nematic $O_{3z^2-r^2}$ order triggers the new C_4 isostructural transition at $x \sim 0.5$ [17]. Also, we obtained the approximate s_{++}-wave gap structure due to orbital fluctuations for both $x \gtrsim 0$ and $x \lesssim 0.5$ by taking the Δ-VC into account. The switch of the dominant quadrupole fluctuations in Fig. 2 gives the minimum structure of T_c around $x \sim 0.2$. The non-nematic orbital fluctuations will be a key ingredient in realizing high T_c (~50 K) in H-doped La1111, Sm1111, as well as Ca122.

We are grateful to H. Hosono, J. Yamaura, Y. Murakami, N. Fujiwara, H. Hiraga, and S. Iimura for useful discussions. This study has been supported by Grants-in-Aid for Scientific Research from MEXT of Japan.

[1] Y. Mizuguchi and Y. Takano, J. Phys. Soc. Jpn. **79**, 102001 (2010).
[2] R. M. Fernandes, L. H. VanBebber, S. Bhattacharya, P. Chandra, V. Keppens, D. Mandrus, M. A. McGuire, B. C. Sales, A. S. Sefat, and J. Schmalian, Phys. Rev. Lett. **105**, 157003 (2010).

[3] F. Krüger, S. Kumar, J. Zaanen, and J. van den Brink, Phys. Rev. B **79**, 054504 (2009).

[4] W. Lv, J. Wu, and P. Phillips, Phys. Rev. B **80**, 224506 (2009).

[5] C.-C. Lee, W.-G. Yin, and W. Ku, Phys. Rev. Lett. **103**, 267001 (2009).

[6] S. Onari and H. Kontani, Phys. Rev. Lett. **109**, 137001 (2012).

[7] S. Liang, A. Moreo, and E. Dagotto, Phys. Rev. Lett. **111**, 047004 (2013).

[8] M. Yoshizawa, D. Kimura, T. Chiba, S. Simayi, Y. Nakanishi, K. Kihou, C. -H. Lee, A. Iyo, H. Eisaki, M. Nakajima, and S. Uchida, J. Phys. Soc. Jpn. **81**, 024604 (2012).

[9] A. E. Böhmer, P. Burger, F. Hardy, T. Wolf, P. Schweiss, R. Fromknecht, M. Reinecker, W. Schranz, and C. Meingast, Phys. Rev. Lett. **112**, 047001 (2014).

[10] M. Yi, D. Lu, J.-H. Chu, J. G. Analytis, A. P. Sorini, A. F. Kemper, B. Moritz, S.-K. Mo, R. G. Moore, M. Hashimoto, W.-S. Lee, Z. Hussain, T. P. Devereaux, I. R. Fisher, and Z.-X. Shen, Proc. Natl. Acad. Sci. U.S.A. **108**, 6878 (2011).

[11] T. Shimojima *et al.*., Phys. Rev. B **89**, 045101 (2014).

[12] Y. Gallais, R. M. Fernandes, I. Paul, L. Chauviere, Y.-X. Yang, M.-A. Measson, M. Cazayous, A. Sacuto, D. Colson, and A. Forget, Phys. Rev. Lett. **111**, 267001 (2013).

[13] H. Kontani and Y. Yamakawa, arXiv:1312.0528.

[14] S. Kasahara, H. J. Shi, K. Hashimoto, S. Tonegawa, Y. Mizukami, T. Shibauchi, K. Sugimoto, T. Fukuda, T. Terashima, A. H. Nevidomskyy, and Y. Matsuda, Nature (London) **486**, 382 (2012).

[15] S. Iimura, S. Matuishi, H. Sato, T. Hanna, Y. Muraba, S. W. Kim, J. E. Kim, M. Takata, and H. Hosono, Nat. Commun. **3**, 943 (2012).

[16] N. Fujiwara, S. Tsutsumi, S. Iimura, S. Matsuishi, H. Hosono, Y. Yamakawa, and H. Kontani, Phys. Rev. Lett. **111**, 097002 (2013).

[17] M. Hiraishi *et al.*, Nat. Phys. **10**, 300 (2014).

[18] For $x > 0.5$, in addition to the c-axis length change, Fe layers and As layers slide alternatively at T_S [17]. The latter may be due to a band Jahn-Teller effect since the lattice deformation is very large.

[19] S. R. Saha, N. P. Butch, T. Drye, J. Magill, S. Ziemak, K. Kirshenbaum, P. Y. Zavalij, J. W. Lynn, and J. Paglione, Phys. Rev. B **85**, 024525 (2012).

[20] K. Kudo, K. Iba, M. Takasuga, Y. Kitahama, J. Matsumura, M. Danura, Y. Nogami, and M. Nohara, Sci. Rep. **3**, 1478 (2013).

[21] S. Avci, O. Chmaissem, S. Rosenkranz, J. M. Allred, I. Eremin, A. V. Chubukov, D.-Y. Chung, M. G. Kanatzidis, J.-P. Castellan, J. A. Schlueter, H. Claus, D. D. Khalyavin, P. Manuel, A. Daoud-Aladine, and R. Osborn, arXiv:1303.2647

[22] Y. Yamakawa, S. Onari, H. Kontani, N. Fujiwara, S. Iimura, and H. Hosono, Phys. Rev. B **88**, 041106(R) (2013).

[23] K. Suzuki, H. Usui, K. Kuroki, S. Iimura, Y. Sato, S. Matsuishi, and H. Hosono, J. Phys. Soc. Jpn. **82**, 083702 (2013).

[24] K. Suzuki, H. Usui, S. Iimura, Y. Sato, S. Matsuishi, H. Hosono, and K. Kuroki, arXiv:1311.2413.

[25] S. Simayi, K. Sakano, H. Takezawa, M. Nakamura, Y. Nakanishi, K. Kihou, M. Nakajima, C. Lee, A. Iyo, H. Eisaki, S. Uchida, and M. Yoshizawa, J. Phys. Soc. Jpn. **82**, 114604 (2013).

[26] A. O. Sboychakov, A. V. Rozhkov, K. I. Kugel, A. L. Rakhmanov, and F. Nori, Phys. Rev. B **88**, 195142 (2013).

[27] H. Kontani and S. Onari, Phys. Rev. Lett. **104**, 157001 (2010).

[28] Y. Ohno, M. Tsuchiizu, S. Onari, and H. Kontani, J. Phys. Soc. Jpn. **82**, 013707 (2013).

[29] M. Tsuchiizu, Y. Ohno, S. Onari, and H. Kontani, Phys. Rev. Lett. **111**, 057003 (2013).

[30] The nonzero matrix elements of $\hat{O}_\gamma$ with respect to 2–4 orbitals are $O^{2,2}_{x^2-y^2} = -O^{3,3}_{x^2-y^2} = 1$, $2O^{2,2}_{3z^2-r^2} = 2O^{3,3}_{3z^2-r^2} = -O^{4,4}_{3z^2-r^2} = 1$, and $O^{3,4}_{xz} = O^{4,3}_{xz} = 1$ [27].

[31] T. Saito, S. Onari, Y. Yamakawa, H. Kontani, S. V. Borisenko, and V. B. Zabolotnyy, arXiv:1402.2398.

[32] See the Supplemental Material at http://link.aps.org/supplemental/10.1103/PhysRevLett.112.187001 for results by the fluctuation-exchange approximation and the SC-VC$_{(\Sigma)}$ method.

[33] H. Kontani, T. Saito, and S. Onari, Phys. Rev. B **84**, 024528 (2011).

[34] C. Ma, L. Wu, W.-G. Yin, H. Yang, H. Shi, Z. Wang, J. Li, C. C. Homes, and Y. Zhu, Phys. Rev. Lett. **112**, 077001 (2014).

[35] K. I. Kugel and D. I. Khomskii, Sov. Phys. Usp. **25**, 231 (1982).

[36] E. F. Shender, Sov. Phys. JETP **56**, 178 (1982); C. L. Henley, Phys. Rev. Lett. **62**, 2056 (1989); A. Moreo, E. Dagotto, T. Jolicoeur, and J. Riera, Phys. Rev. B **42**, 6283 (1990); P. Chandra, P. Coleman, and A. I. Larkin, Phys. Rev. Lett. **64**, 88 (1990).

[37] C.-Y. Moon and H. J. Choi, Phys. Rev. Lett. **104**, 057003 (2010); W.-G. Yin, C.-C. Lee, and W. Ku, Phys. Rev. Lett. **105**, 1070004 (2010).

[38] T. Saito, S. Onari, and H. Kontani, Phys. Rev. B **88**, 045115 (2013).

[39] A. Kawabata, S. C. Lee, T. Moyoshi, Y. Kobayashi, and M. Sato, J. Phys. Soc. Jpn. **77**, 103704 (2008).

[40] Y. Nakajima, T. Taen, Y. Tsuchiya, T. Tamegai, H. Kitamura, and T. Murakami, Phys. Rev. B **82**, 220504 (2010).

[41] J. Li, Y. F. Guo, S. B. Zhang, J. Yuan, Y. Tsujimoto, X. Wang, C. I. Sathish, Y. Sun, S. Yu, W. Yi, K. Yamaura, E. Takayama-Muromachiu, Y. Shirako, M. Akaogi, and H. Kontani, Phys. Rev. B **85**, 214509 (2012).

[42] S. Onari and H. Kontani, Phys. Rev. Lett. **103**, 177001 (2009).

[43] Y. Yamakawa, S. Onari, and H. Kontani, Phys. Rev. B **87**, 195121 (2013).

[44] Y. Wang, A. Kreisel, P. J. Hirschfeld, and V. Mishra, Phys. Rev. B **87**, 094504 (2013); They reported that the conventional $s_\pm$-wave state becomes very robust against the unitary scatters since they used an oversimplified two-band model. This artifact due to the oversimplified model is explained in Sec. VC of Ref. [43] in detail.

[45] K. Kuroki, S. Onari, R. Arita, H. Usui, Y. Tanaka, H. Kontani, and H. Aoki, Phys. Rev. Lett. **101**, 087004 (2008).

[46] P. J. Hirschfeld, M. M. Korshunov, and I. I. Mazin, Rep. Prog. Phys. **74**, 124508 (2011).

[47] A. V. Chubukov, D. V. Efremov, and I. Eremin, Phys. Rev. B **78**, 134512 (2008).

[48] S. Matsuishi, T. Maruyama, S. Iimura, and H. Hosono, Phys. Rev. B **89**, 094510 (2014).